*Acta Oceanol. Sin.*, 2021, Vol. 40, No. 3, P. 70–83
https://doi.org/10.1007/s13131-021-1711-8
http://www.hyxb.org.cn
E-mail: hyxbe@263.net

# Tectonic implications of the subduction of the Kyushu-Palau Ridge beneath the Kyushu, southwest Japan

Chenglong Xia[1, 2], Yanpeng Zheng[2, 3*], Baohua Liu[2, 4], Qingfeng Hua[2, 5], Long Ma[2, 5], Xianfeng Li[2, 5], Qiuhong Xie[2, 5]

[1] College of Marine Geosciences, Ocean University of China, Qingdao 266100, China

[2] Laboratory for Marine Geology, Pilot National Laboratory for Marine Science and Technology (Qingdao), Qingdao 266237, China

[3] Hubei Key Laboratory of Marine Geological Resources, China University of Geosciences, Wuhan 430074, China

[4] National Deep Sea Center, Qingdao 266237, China

[5] Key Laboratory of Marine Geology and Metallogeny, First Institute of Oceanography, Ministry of Natural Resources, Qingdao 266061, China

Received 7 July 2020; accepted 30 July 2020



**Abstract**

The Kyushu-Palau Ridge (KPR), a remnant arc on the Philippine Sea Plate (PSP), is subducting beneath the Kyushu, southwest Japan. Influenced by the subducting KPR, the Kyushu subduction zone corresponding to the KPR is significantly different from Shikoku subduction zone in terms of gravity anomalies, seismicity, the stress state, and the subducting slab morphology. Significant negative free-air and Bouguer gravity anomalies are observed in a prolonged area of KPR, southeast of the Miyazaki Plain, indicating that this is where KPR overlaps the overriding plate. The gravity anomaly in this area is much lower than that in other areas where the inferred KPR extends, suggesting that the subduction of the buoyant KPR may cause the lower mantle density to decrease. More earthquakes have occurred in Hyuga-nada region where the KPR subducts than in Shikoku forearc and other areas in the Kyushu forearc, indicating that the subduction of the KPR enhances the local coupling between the subducting and overriding plates. The centroid moment tensor (CMT) mechanism of earthquakes shows that stress is concentrated in the accumulated crust beneath the Kyushu forearc corresponding to the KPR, and the shallow thrusting events in the obducting plate are caused by the KPR subduction. The buoyant KPR, with a large volume of low-density sediments, was responsible for the differences of the subduction depth and dip angle of the subducting Philippine Sea (PS) slab between northern Kyushu and Shikoku. The seismic gaps and the sudden change of the dipping angle of the subducting PS slab indicate that slab tear may have occurred along the west side of the KPR beneath southwest Kyushu. A two-tear model was proposed, and the subduction of the buoyant KPR was believed to play an important role in the slab tear.

**Key words:** Kyushu-Palau Ridge, gravity anomaly, seismicity, slab morphology, slab tear

**Citation:** Xia Chenglong, Zheng Yanpeng, Liu Baohua, Hua Qingfeng, Ma Long, Li Xianfeng, Xie Qiuhong. 2021. Tectonic implications of the subduction of the Kyushu-Palau Ridge beneath the Kyushu, southwest Japan. Acta Oceanologica Sinica, 40(3): 70–83, doi: 10.1007/s13131-021-1711-8

## 1 Introduction

Bathymetric highs on subducting oceanic crust (such as aseismic ridges and seamount chains) have significant effects on the morphology of the subducting slab, and the geological and geophysical characteristics of the subduction zone (Das and Watts, 2009; Mason et al., 2010; Yan and Shi, 2014). The Kyushu-Palau Ridge (KPR) is a north-south-oriented bathymetric high situated atop the Philippine Sea Plate (PSP). Geomorphology (Nakada et al., 2002), tomography (Tahara et al., 2008), and multichannel seismic reflection profile studies (Nishizawa et al., 2009) illustrate that the KPR is being thrust beneath the southwest Japan in the Hyuga-nada region, that is, the western extent of the Nankai Trough subduction zone. The subduction of the KPR has resulted in strong deformation of the Kyushu forearc crust and has caused significant crustal uplift in the Miyazaki Plain (Nakada et al., 2002; Park et al., 2009). GPS measurement data of horizontal displacements shows that the inter-plate coupling along the Nankai Trough is strong in Shikoku and weak in Kyushu (Nishimura et al., 1999). However, more earthquakes have occurred in the Hyuga-nada region than Shikoku forearc since the 1960s, especially in the Kyushu forearc corresponding to the KPR.

Foundation item: The Natural Science Foundation of China-Shandong Joint Fund for Marine Science Research Centers under contract No. U1606401; the Scientific and Technological Innovation Project financially supported by the Pilot National Laboratory for Marine Science and Technology (Qingdao) under contract No. 2016ASKJ13; the Deep Sea Observation-Techniques and Equipments Development under contract No. 2016ASKJ15; the Taishan Scholar Project Funding under contract No. tspd20161007; the National Natural Science Foundation of China under contract No. 41606084; the National Programme on Global Change and Air-Sea Interaction under contract No. GASI-GEOGE-02.

*Corresponding author, E-mail: zhengyanpeng@cug.edu.cn

Adakites are usually formed by the direct melting of young (<25 Ma) and hot subducting slabs (Defant and Drummond, 1990). In general, in the case of the formation of a slab window, the edge of the slab is heated or melted by the mantle to produce adakites, and the distribution of adakitic magmas can approximately indicate the geometric boundary of the subducting plate (Yogodzinski et al., 2001). A large number of adakites have been found in southwest Japan (Morris, 1995; Kakubuchi et al., 2000; Sugimoto et al., 2006; Mahony et al., 2011). Geochemical evidence shows that the adakites that have erupted in northeast Kyushu and southwest Honshu are chemically similar to the composition of the PSP; hence, these adakites are believed to have been formed by the melting of the PSP beneath southwest Japan (Morris, 1995; Kimura et al., 2003). The heat required to melt the oceanic crust may originate from a slab window, the formation of which is related to slab separation or tearing of the slab. The collision between a bathymetric high and a trench is an important factor that leads to arcuate development of the trench and tearing of the subducted slab (Bautista et al., 2001; Mason et al., 2010). Slab tear also occurred in the Manila subduction zone (Fan et al., 2015, 2016), the southern end of the Ogasawara subduction zone (Castle and Creager, 1998, 1999; Miller et al., 2004; Kong et al., 2017), and the North Andean margin (Gutscher et al., 1999), which are considered to be affected by the subduction of the ancient spreading ridge of the South China Sea, the Ogasawara plateau, and the Carnegie Ridge, respectively. Cao et al. (2014) confirmed the observation by Zhao et al. (2012) that the P-wave high-velocity anomaly is apparently interrupted by a low-velocity anomaly beneath southwest Honshu and Kyushu. Huang et al. (2013) and Cao et al. (2014) believed that the Philippine Sea slab is tearing and forms a slab window that corresponds to the KPR due to the subduction of the buoyant KPR and the motion change of the PSP.

The slab window beneath Kyushu and the western Honshu, however, cannot explain why adakites are found in southwest Kyushu. In addition, most of the adakites related to ridge subduction are closely related to the genesis of the porphyry Cu-Au deposits in the circum Pacific tectonic zone (Peacock et al., 1994; Thiéblemont et al., 1997; Sajona and Maury, 1998; Defant et al., 2001; Oyarzun et al., 2001; Mungall, 2002; Sun et al., 2011). The genesis of the low-sulfidation epithermal gold deposits in Hishikari (Izawa et al., 1990; Cooke and Simmons, 2000), high-sulfidation gold deposits in Nansatsu (Hedenquist et al., 1994; Cooke and Simmons, 2000), and porphyry deposits that may be present but remain unexposed in southwest Kyushu still cannot be explained by the slab window under the northeast Kyushu. Cooke et al. (2005) proposed that the gold deposits in southwest Kyushu may be related to the low-angle subduction of the KPR. However, the tectonic genesis of these gold deposits remain unclear.

In this paper, the gravity anomalies and seismicity of the Kyushu and Shikoku, and the morphology of the subducting Philippine Sea (PS) slab beneath Kyushu and Shikoku are described. By comparing the geological and geophysical differences between the Shikoku subduction zone and the Kyushu subduction zone corresponding to the KPR, the tectonic significance of KPR subduction under Kyushu is revealed.

## 2 Tectonic setting

The KPR, which extends north-south from the southeast Kyushu to the Palau Islands (Fig. 1a), is a remnant island arc that was separated from the proto-Izu-Bonin-Mariana (IBM) arc after

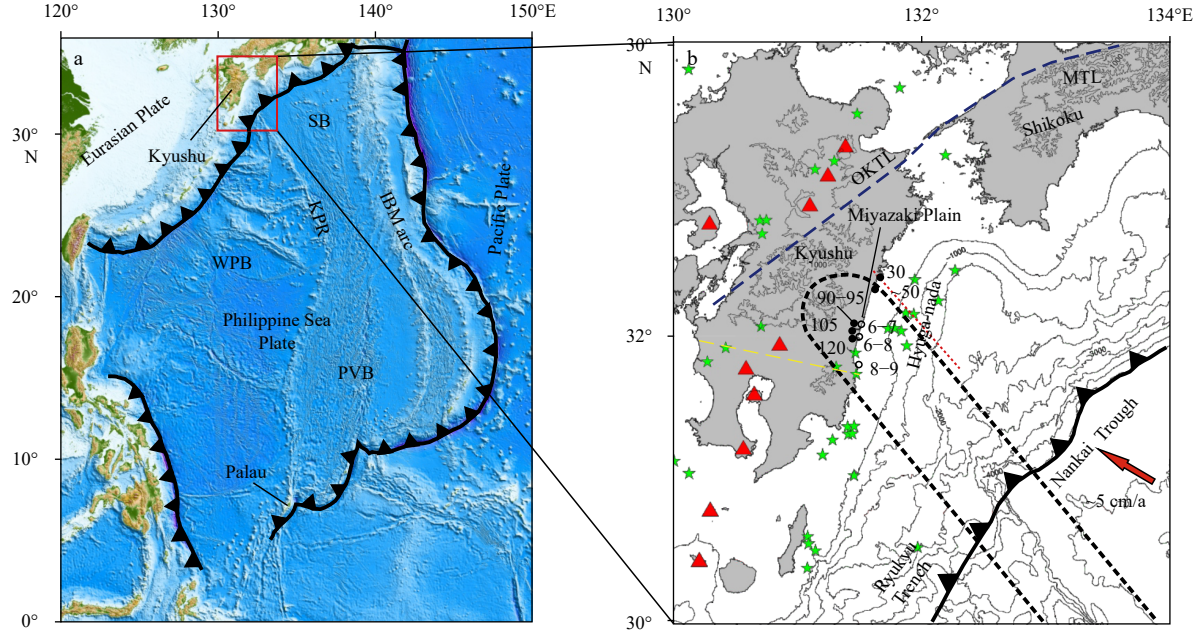


**Fig. 1.** Overview of the plate tectonics of the southwestern Japan. The topography is from ETOPO1 (Amante and Eakins, 2009). The red triangles represent active volcanoes. Intermediate-magnitude ($6 \leqslant M_W \leqslant 7.5$) earthquakes that have occurred in the Hyuga-nada region since the 1960s are marked with green stars. The yellow and blue dashed lines denote the active left-lateral shear zone and tectonic line, respectively. The black dashed line demarcates the inferred subducted KPR, and the red dotted line shows the location of the slab fracture (Park et al., 2009). The sawtooth curves represent the trenches. The solid and open circles denote uplifted marine terraces formed during the late Pleistocene and middle Holocene, respectively (Nakada et al., 2002). The altitudes of these terraces (m) are also shown. WPB: West Philippine Basin, SB: Shikoku Basin, PVB: Parece Vela Basin, KPR: Kyushu-Palau Ridge, OKTL: Oita-Kumamoto Tectonic Line, and MTL: Median Tectonic Line.

the spreading of the Shikoku Basin and the Parece Vela Basin (Karig, 1972; Ishizuka et al., 2011; Lallemand, 2016). The overall topography of the KPR, which is approximately 2 600 km long and approximately 90 km wide, is steep to the east and gentle to the west. The water depth at the peak of the ridge is between 2 000 m and 4 000 m, while that at the base of the ridge reaches up to 5 000–6 000 m. Radiometric ages of samples collected from the KPR range in age between 43 Ma and 25 Ma, mostly between 27 Ma and 25 Ma (Expedition 351 Scientists, 2015), indicating that arc volcanism within the KPR ended during the late Oligocene. In addition, the petrology and geochemistry of rocks collected from the KPR indicate that the ridge is composed mainly of intraoceanic tholeiite (Ishizuka et al., 2011). The crustal thickness of the KPR varies greatly, generally between 10 km and 20 km (Ishihara and Koda, 2007; Nishizawa et al., 2007, 2009; Zhang et al., 2012), but the absence of the middle crust from the middle segment of the KPR indicates that it is an immature volcanic arc (Yan and Shi, 2011). The northern segments of the KPR form the western boundary of a late Oligocene to Miocene basin and eastern boundary of a complex array of Cretaceous to Eocene ridges and basins (Fig. 1).

The proto-IBM arc began to form at 50–45 Ma (Cosca et al., 1998; Deschamps and Lallemand, 2002; Hall et al., 2003; Gurnis et al., 2004) and was completely formed by approximately 35 Ma (Haraguchi et al., 2003). Due to the continuous subduction of the Pacific Plate, the proto-IBM trench experienced rollback, and thus, the proto-IBM arc began to rift. Subsequently, spreading occurred within the Shikoku Basin and the Parece Vela Basin between 30 Ma and 15 Ma (Seno and Maruyama, 1984; Okino et al., 1994; Xia et al., 2017) and between 29 Ma and 12 Ma (Okino et al., 1999; Sdrolias et al., 2004), respectively. As a result, the KPR began to subduct with the PSP beneath the Eurasian Plate in the late Miocene (Kimura, 1996). According to the velocity model of DeMets et al. (2010) ((58.4±1.2) mm/a), this results in nearly 400 km of the KPR being lost by subduction at the Nankai Trough.

The Kyushu forearc where the KPR suducts displays a disturbed seafloor topography compared with the forearc wedge off the Shikoku. Strong deformation of the forearc sedimentary layers can be inferred from the crustal velocity models (Ichikawa, 1997). In addition, the eastern part of Kyushu, especially the Miyazaki Plain, experienced significant uplift during the late Pleistocene and Holocene (Fig. 1b), and accordingly, a large number of marine terraces are developed at elevations of 30–120 m (Nagaoka, 1986; Shimoyama et al., 1999). Moreover, the counterclockwise rotation of southern Kyushu (up to 30°) is documented by paleomagnetic declinations over the past 2 Ma (Kodama et al., 1995). The abovementioned geological phenomena may be related to the subduction of the KPR.

The PSP rotated nearly 50° clockwise between 50 Ma and 40 Ma and 34° clockwise between 15 Ma and 5 Ma (Hall, 2002). However, the PSP has rotated only 5.5° since 5 Ma (Hall et al., 1995a, b, c), and the current rotational speed of the PSP is approximately 1°/Ma (Sella et al., 2002). Hence, it is possible that the slowing rotational speed of the PSP may be related to the obstruction of the KPR.

## 3 Gravity anomaly and seismicity

### 3.1 *Data*

The free-air gravity data used in this study were derived from the latest, most influential and widely used satellite gravity data with a resolution of 1 arcminute (Smith and Sandwell, 1997; Sandwell et al., 2014) published by the Scripps Institute of Oceanography, University of California, San Diego. The Bouguer gravity anomaly was calculated using seafloor topography information from the ETOPO1 global database (Amante and Eakins, 2009) and the free-air gravity anomaly derived from satellite altimetry. The Bouguer gravity correction was based on a three-dimensional terrain correction with an assumed crustal density of 2 670 kg/m$^3$ and a seawater density of 1 030 kg/m$^3$.

For this study area, 1 278 events (magnitude $M_W \geqslant 3$) from January 1960 to January 2018 were obtained from the United States Geological Survey (USGS) Earthquake Hazards Program. In addition, centroid moment tensor (CMT) data were downloaded from the Harvard Global CMT (GCMT) catalog (Dziewonski et al., 1981; Ekström et al., 2012).

### 3.2 *Gravity anomaly*

The free-air gravity anomalies in Kyushu and its vicinity range between $-150\times10^{-5}$ m/s$^2$ and $215\times10^{-5}$ m/s$^2$ (Fig. 2a). The main islands of Kyushu and Shikoku show obvious positive anomalies. The most prominent gravity anomaly over the entire region is the maximum negative anomaly off the Miyazaki Plain, where the anomaly drops below $-150\times10^{-5}$ m/s$^2$. Moreover, while the free-air gravity anomalies throughout the Shikoku forearc show positive values ranging from 0 m/s$^2$ to $50\times10^{-5}$ m/s$^2$, the negative gravity anomalies along the western margin of the Nankai Trough show little change with values ranging mainly from $-50\times10^{-5}$ m/s$^2$ to 0.

The Bouguer anomalies in the study area exhibit linearity with a NE-SW orientation, and the anomaly contours roughly follow the trench and forearc structures (Fig. 2b). The Bouguer anomalies of the Nankai Trough in the Shikoku segment are relatively high. The gravity high along the outer edge of the Nankai Trough appears as a NE-SW strip. The Kyushu forearc is characterized by negative anomalies on a large scale, and a negative Bouguer anomaly depression occurs at 31°54′N, 131°48′E in the Hyuga-nada where the KPR subducts, which coincided with the maximum negative free-air gravity anomaly.

### 3.3 *Seismicity and subducting slab morphology*

#### 3.3.1 *Seismicity*

The regional distribution characteristics of earthquakes with different depths can be obtained through a map of the epicenter distribution (Fig. 3). Relatively few earthquakes are observed at the junction between the KPR and Nankai Trough, but an increasing trend in the direction of the island arc is noted.

The focal depths of the earthquakes in Kyushu are basically within 200 km, where shallow earthquakes account for 81% of all events, as deep earthquakes are missing. Earthquakes with focal depths of 0–30 km are distributed mainly in the subduction zone and in central and southern Kyushu. The seismic belt traversing the central part of Kyushu extends NE-SW. It is worth noting that this seismic belt is located within the region of extension corresponding to the central tectonic belt in Kyushu, which may indicate that the earthquakes occurring here are related to the right-lateral shear of this tectonic belt. In contrast, the earthquakes in the southern Kyushu are distributed in nearly east-west, corresponding to the left-lateral shear zone spreading east-west in southern Kyushu. In addition, earthquakes with focal depths of 30–80 km are concentrated mainly in the Kyushu forearc. Finally, earthquakes with focal depths of 80–160 km occur along a linear trend oriented NE-SW through central Kyushu, while earthquakes with a focal depth greater than 160 km occur only beneath the central and southern Kyushu.

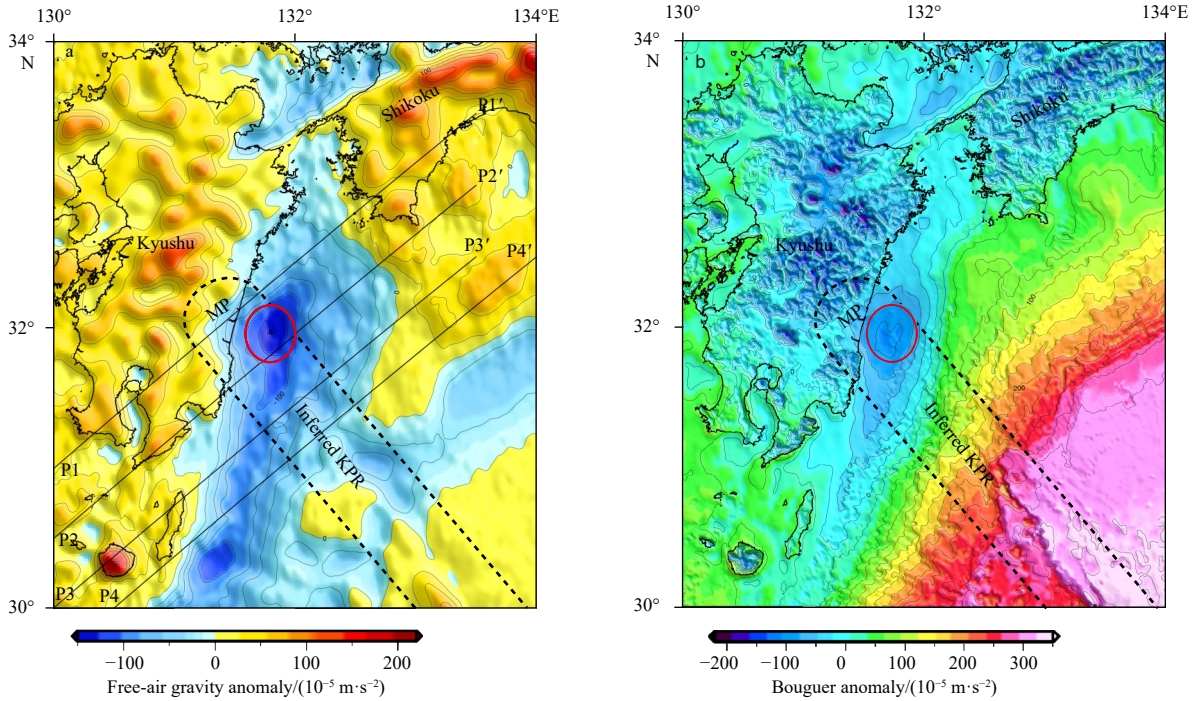


**Fig. 2.** Free-air gravity anomaly map of the study area (a), and Bouguer anomaly map of the study area (b). The contours represent intervals of $25\times10^{-5}$ m/s$^2$. The red ellipses mark the maximum negative gravity anomalies off the Miyazaki Plain. Lines with capital letters (e.g., P1–P1′) are the positions of the geophysical sections shown in Fig. 7. MP: Miyazaki Plain.

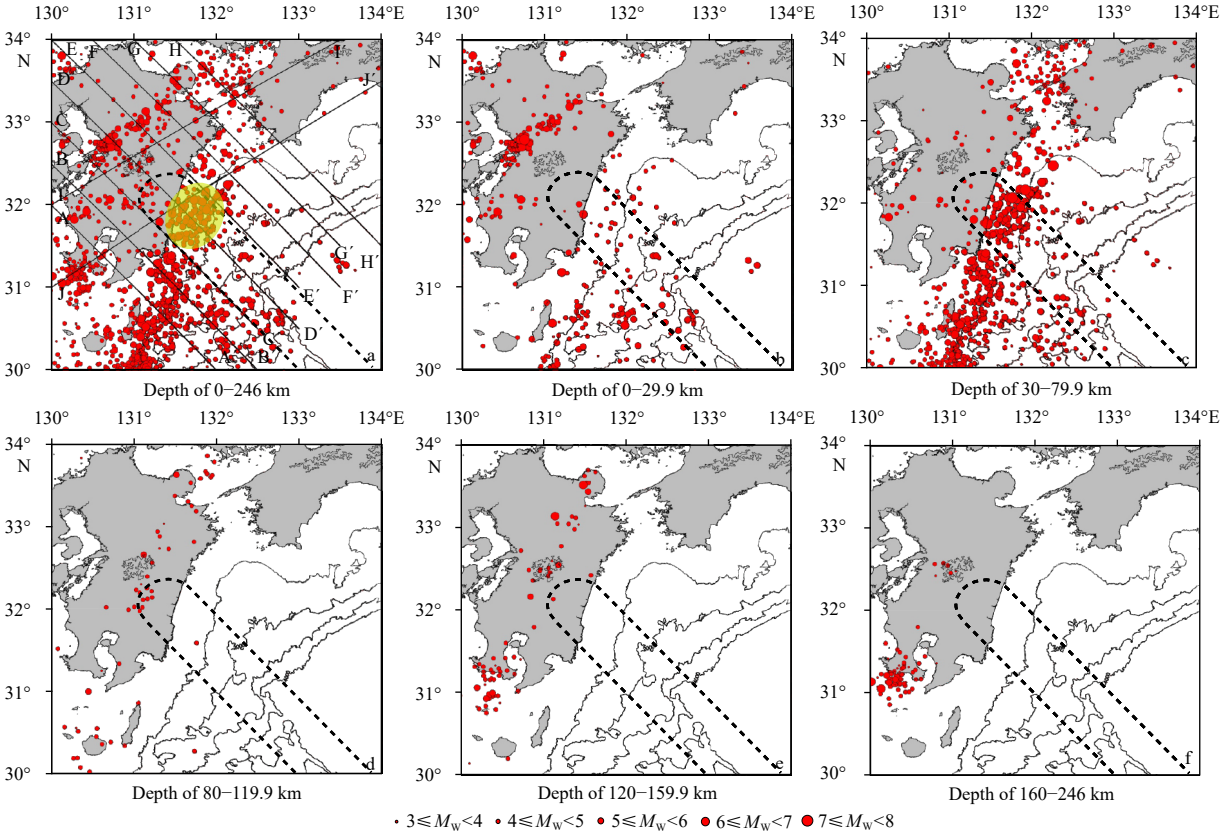


**Fig. 3.** Epicentral distribution of earthquakes ($M_W\geq3$) in different depth ranges for southwest Japan from 1960 to 2018. Earthquake epicenters were derived from the USGS Earthquake Hazards Program. Lines with capital letters (e.g., A–A′) are the positions of the seismicity profiles shown in Fig. 5. The light yellow ellipse denotes the seismic concentration zone in Hyuga-nada region.

There is an earthquake cluster in Hyuga-nada region, especially above the KPR (Fig. 3a). According to the seismic data collected by the USGS, 50% of the earthquakes with a magnitude greater than 6 that occurred in Hyuga-nada since the 1960s were concentrated in the area overlying the inferred area of the subducting KPR; this is especially true for earthquakes of magnitude 7 or higher, all of which occurred in this area (Fig. 3).

3.3.2 *Focal mechanism*

A total of 131 fault plane solutions for the study area were acquired from the GCMT catalog (Dziewonski et al., 1981; Ekström et al., 2012) for the period from January 1976 to January 2018. A representative subset comprising 42 of these events is listed in Table 1 and shown in Fig. 4. In general, the mechanisms are consistent with the plate tectonic model of the study area. Several principal types of focal mechanisms can be distinguished: (1) shallow dextral strike-slip events occurring along the Oita-Kumamoto Tectonic Line (Events 1–5); (2) shallow left-lateral strike-slip events in the active left-lateral shear zone (6–9); (3) shallow normal faulting events in the subduction zone (10–27); (4) shallow thrusting events in the obducting plate due to the subduction of the KPR (28–35); and (5) deep underthrusting-induced events in the downgoing slab (36–42).

3.3.3 *Morphology of the subducting PS slab*

The Wadati-Benioff zone constitutes an important basis for studying the morphological characteristics of any subduction zone (Zang and Ning, 1996). By extracting the earthquakes along

**Table 1.** List of the events and fault plane solutions obtained from the GCMT catalog

| Event No. | Date (d/m/y) | Time (GMT) | N lat/(°) | E lon/(°) | Depth/km | $M_W$ | Mb | Ms | Fault plane 1 strike/ dip/slip /(°) | Fault plane 2 strike/ dip/slip /(°) |
|---|---|---|---|---|---|---|---|---|---|---|
| 1 | 14/4/2016 | 15:03 | 32.71 | 130.69 | 12.0 | 6.0 | 0.0 | 6.0 | 30/77/180 | 120/90/13 |
| 2 | 18/4/2016 | 11:42 | 33.00 | 131.12 | 13.2 | 5.5 | 0.0 | 5.5 | 44/79/–175 | 313/85/–11 |
| 3 | 19/4/2016 | 08:52 | 32.55 | 130.54 | 13.3 | 5.3 | 0.0 | 5.3 | 36/73/–177 | 305/87/–17 |
| 4 | 19/4/2016 | 11:47 | 32.62 | 130.56 | 16.1 | 4.9 | 0.0 | 4.8 | 21/77/179 | 112/89/13 |
| 5 | 5/5/2016 | 01:40 | 33.02 | 130.92 | 24.4 | 4.9 | 0.0 | 4.6 | 49/60/–179 | 318/89/–30 |
| 6 | 12/2/1994 | 17:07 | 32.03 | 130.33 | 15.0 | 5.4 | 4.7 | 5.3 | 179/89/–179 | 89/89/–1 |
| 7 | 26/3/1997 | 08:31 | 32.04 | 130.09 | 29.8 | 6.1 | 5.6 | 5.9 | 8/89/179 | 98/89/1 |
| 8 | 2/4/1997 | 19:33 | 31.82 | 130.17 | 15.0 | 5.4 | 5.1 | 5.0 | 2/70/166 | 97/77/20 |
| 9 | 13/5/1997 | 05:38 | 32.00 | 130.26 | 16.2 | 6.0 | 5.6 | 5.8 | 280/75/–14 | 14/77/–164 |
| 10 | 5/12/1983 | 01:53 | 32.29 | 131.64 | 31.5 | 5.4 | 5.0 | 5.5 | 340/9/–151 | 221/86/–82 |
| 11 | 6/8/1984 | 19.06 | 32.34 | 131.94 | 28.5 | 6.9 | 6.2 | 6.8 | 337/7/–136 | 203/85/–85 |
| 12 | 12/5/1985 | 10:41 | 32.83 | 132.52 | 38.9 | 5.5 | 5.7 | 5.2 | 0/33/–103 | 195/58/–82 |
| 13 | 18/3/1987 | 03:36 | 31.94 | 131.77 | 38.0 | 6.0 | 6.5 | 6.6 | 348/27/–103 | 182/64/–84 |
| 14 | 27/3/2006 | 02:50 | 32.70 | 132.02 | 22.2 | 5.5 | 5.3 | 5.7 | 315/5/–164 | 09/89/–85 |
| 15 | 5/8/2009 | 03:51 | 32.56 | 131.97 | 33.4 | 5.0 | 5.1 | 0.0 | 360/25/–90 | 180/65/–90 |
| 16 | 2/3/2017 | 14:53 | 32.69 | 131.82 | 48.7 | 5.2 | 0.0 | 5.3 | 334/25/–129 | 196/71/–74 |
| 17 | 30/6/1984 | 20:27 | 30.07 | 131.47 | 23.8 | 5.4 | 5.3 | 0.0 | 348/38/–107 | 189/54/–78 |
| 18 | 2/3/1985 | 08:45 | 30.54 | 132.15 | 17.9 | 5.3 | 5.3 | 5.1 | 6/32/–100 | 197/59/–84 |
| 19 | 27/9/1993 | 04:43 | 30.81 | 132.21 | 27.0 | 5.6 | 5.5 | 5.2 | 36/26/–55 | 177/69/–105 |
| 20 | 14/11/1995 | 17:08 | 31.48 | 133.10 | 28.8 | 5.0 | 5.1 | 4.2 | 199/45/–81 | 6/45/–99 |
| 21 | 16/7/2002 | 11:57 | 30.87 | 132.35 | 15.0 | 5.4 | 5.4 | 4.8 | 21/45/–70 | 173/48/–109 |
| 22 | 9/4/2011 | 12:57 | 30.04 | 131.84 | 12.2 | 6.0 | 6.1 | 6.0 | 358/36/–107 | 199/56/–78 |
| 23 | 13/2/2013 | 03:57 | 30.30 | 131.58 | 12.0 | 5.4 | 5.5 | 5.4 | 343/26/–134 | 211/72/–71 |
| 24 | 29/42 017 | 12:32 | 30.82 | 131.43 | 25.9 | 5.8 | 0.0 | 5.7 | 355/30/–133 | 201/62/–77 |
| 25 | 18/12/2017 | 23.:28 | 30.78 | 131.76 | 12.0 | 5.1 | 0.0 | 5.2 | 39/14/–63 | 191/77/–97 |
| 26 | 20/12/2017 | 13:40 | 30.77 | 132.14 | 12.0 | 5.5 | 0.0 | 5.5 | 352/42/–119 | 209/54/–66 |
| 27 | 21/12/2017 | 03:40 | 30.85 | 131.90 | 12.0 | 5.0 | 0.0 | 5.1 | 17/20/–98 | 205/70/–87 |
| 28 | 19/10/1996 | 08:31 | 31.82 | 131.89 | 38.8 | 5.5 | 5.4 | 5.0 | 94/22/67 | 38/69/99 |
| 29 | 2/12/1996 | 22:18 | 31.76 | 131.72 | 33.4 | 6.7 | 6.0 | 6.6 | 206/19/80 | 37/71/94 |
| 30 | 16/12/1998 | 00:18 | 31.17 | 131.54 | 27.0 | 6.0 | 5.5 | 5.6 | 198/13/63 | 46/78/96 |
| 31 | 31/5/2005 | 02:04 | 31.35 | 131.69 | 38.0 | 5.7 | 5.5 | 5.3 | 188/32/67 | 34/61/103 |
| 32 | 5/4/2009 | 09:36 | 31.78 | 132.06 | 33.5 | 5.8 | 5.8 | 5.8 | 209/24/89 | 31/66/91 |
| 33 | 11/3/2013 | 09:34 | 31.57 | 131.92 | 28.7 | 5.4 | 5.2 | 0.0 | 186/29/70 | 29/63/101 |
| 34 | 18/7/2015 | 17:13 | 31.16 | 131.64 | 34.7 | 4.8 | 0.0 | 4.7 | 187/35/67 | 34/58/05 |
| 35 | 16/5/2016 | 08:50 | 31.69 | 132.08 | 35.9 | 4.9 | 0.0 | 4.8 | 220/32/97 | 32/58/86 |
| 36 | 5/7/1982 | 08:57 | 30.77 | 130.47 | 119.0 | 5.5 | 5.7 | 0.0 | 304/10/173 | 41/89/80 |
| 37 | 23/9/1992 | 13:38 | 31.14 | 130.16 | 168.5 | 5.7 | 5.8 | 0.0 | 261/24/160 | 9/82/68 |
| 38 | 21/11/2005 | 15:36 | 30.97 | 130.31 | 155.0 | 6.2 | 5.9 | 0.0 | 253/17/159 | 4/84/75 |
| 39 | 3/9/2009 | 13:26 | 31.08 | 130.19 | 168.4 | 6.2 | 5.9 | 6.2 | 241/23/131 | 18/73/74 |
| 40 | 25/7/2012 | 17:20 | 31.05 | 130.37 | 137.6 | 5.0 | 5.0 | 0.0 | 247/38/168 | 347/82/52 |
| 41 | 16/10/2012 | 13: 39 | 31.27 | 130.29 | 182.1 | 5.2 | 5.3 | 0.0 | 212/18/116 | 5/74/82 |
| 42 | 11/3/2013 | 05: 35 | 31.21 | 130.40 | 175.7 | 5.0 | 4.7 | 0.0 | 245/14/148 | 6/83/78 |

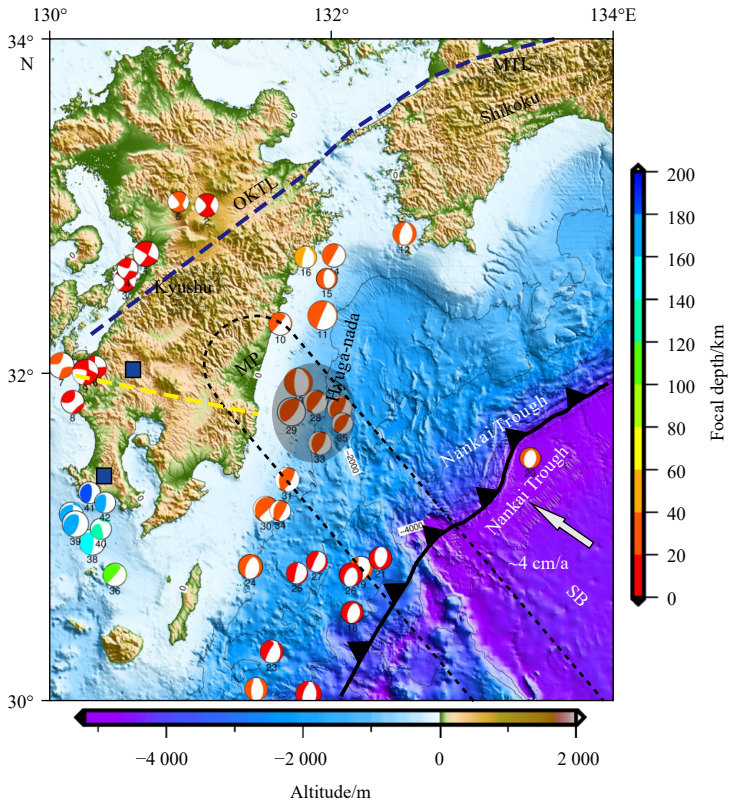


**Fig. 4.** GCMT solutions of earthquakes ($M_W \geq 4$) during 1976–2017. The topography is from SRTM15+ (Tozer et al., 2019). The blue squares show hydrothermal deposits that may be related to the subduction of the KPR. The contours denote the bathymetry at 1 000 m intervals. The size of the focal sphere is proportional to the magnitude of the earthquake, and the color of the compressed quadrant of each focal sphere denotes the depth of the hypocenter. The black dashed line marks the inferred KPR. The light grey ellipse denotes the seismic concentration zone. SB: Shikoku Basin, MP: Miyazaki Plain, MTL: Median Tectonic Line, and OKTL: Oita-Kumamoto Tectonic Line.

cross-sections perpendicular to the strike of the subduction zone, the two-dimensional distributions of the earthquakes in different areas of the subduction zone with respect to the profile distance and depth can be obtained. Many of the slab earthquakes in SW Japan are interpreted as having occurred within the subducted oceanic crust (Wang et al., 2004). Thus, the distributions of seismicity can reflect the morphological characteristics of the subducting PS slab.

To better reveal the characteristics of the subducting PS slab in different regions of southwest Japan, eight cross-sections are constructed perpendicular to the strike of the subduction zone, and two cross-sections are constructed parallel to the strike of the subduction zone. The locations of the cross-sections and the distributions of the earthquakes are shown in Figs 3 and 5. Furthermore, the upper boundary of the subducting slab beneath southwest Japan is delineated in the image on the basis of the slab model (Slab 1.0), which is a three-dimensional compilation of global subduction geometries based on a probabilistic non-linear fit to several data catalogs such as CMT solutions, historic earthquakes, active seismic profiles, bathymetry and sediment thickness (Hayes et al., 2012).

The heterogeneity of the earthquake revealed the difference in the geometry of the subduction slab below Kyushu and Shikoku. The depth of the upper boundary of the subducting PS slab below southwest Japan gradually becomes shallower from west to east and gradually changes from 430 km west of Kyushu to 190 km in the Japan Sea (Figs 5 and 6a). The subducting PS slab shows a sudden change in its subduction depth from 20–50 km under Shikoku to 50–300 km under northern Kyushu. The dip angle of the PS slab also changes from 10°–25° under Shikoku to 25°–65° under northern Kyushu (Fig. 6b).

It is worth noting that on both sides of the inferred KPR, the subduction depth and subduction angle have changed significantly, especially on the northeastern flank (Fig. 6). Moreover, it can be observed that the subduction angle of the Philippine slab is obviously slowed at the Hyuganada region where the KPR subducts, which may be related to the thick and buoyant KPR. Seismic gaps were observed at depths of 200 km and 100 km west of the prolonged area of KPR along cross-sections I–I′ and J–J′ parallel to the strike of the subduction zone, respectively. Seismic gaps are also reflected in Sections A–A′, B–B′, and C–C′ at a depth of 80–100 km (Fig. 5).

## 4 Discussion

### 4.1 *Response of gravity anomaly and seismicity to KPR subduction*

The Shikoku Basin subducted beneath the northern Kyushu and Shikoku along the Nankai Trough. However, the northern part of the Kyushu subduction zone and Shikoku subduction zone show significant geological and geophysical differences, especially in terms of gravity and seismicity.

The free-air anomaly reflects the differences in the shape and

mass distribution between the actual Earth and Earth ellipsoid, thereby reflecting the change trend of the bathymetry. However, the bathymetry in the study area is not strongly related to the free-air anomaly; in particular, the free-air anomaly is much lower in the Kyushu forearc where the KPR subducts (which is relatively shallow) than that in the Nankai Trough (Fig. 2a). Furthermore, the Shikoku forearc shows positive gravity anomalies, while the Kyushu forearc corresponding to the KPR is characterized by significant negative gravity anomalies, and a negative anomaly depression appears off the Miyazaki Plain. Moreover, the gravity anomaly variations in the Shikoku forearc are relatively flat, whereas the gravity anomaly contours in the Kyushu forearc are relatively dense and vary considerably, especially in the Kyushu forearc where the KPR subducts. These obvious differences in the free-air anomaly indicate that the Kyushu forearc is under the control of the mass distribution of deep structure. Chen et al. (2014) suggested that the negative anomalies in the Kyushu forearc may be related to the relatively thick accumulation of upper crustal material above the subduction zone. Site 296 of the Deep Sea Drilling Project and multi-channel seismic profiles reveal that the sedimentary thickness above northern KPR is nearly 1 km (Karig and Ingle, 1975; Nishizawa et al., 2009). Thus, we believe that the young, buoyant KPR carrying a large volume of low-density sediments is responsible for the low free-air anomalies.

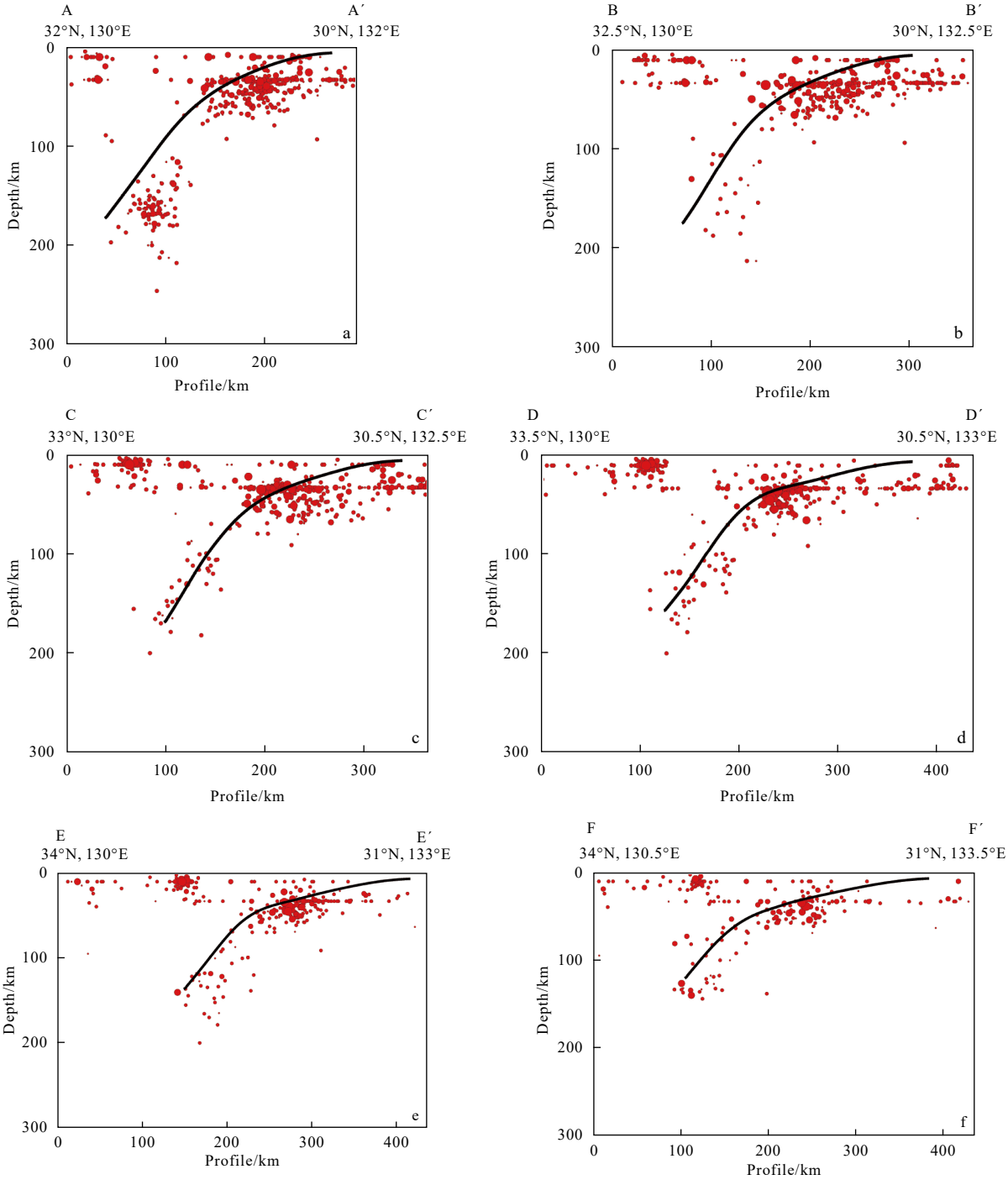


**Fig. 5.**

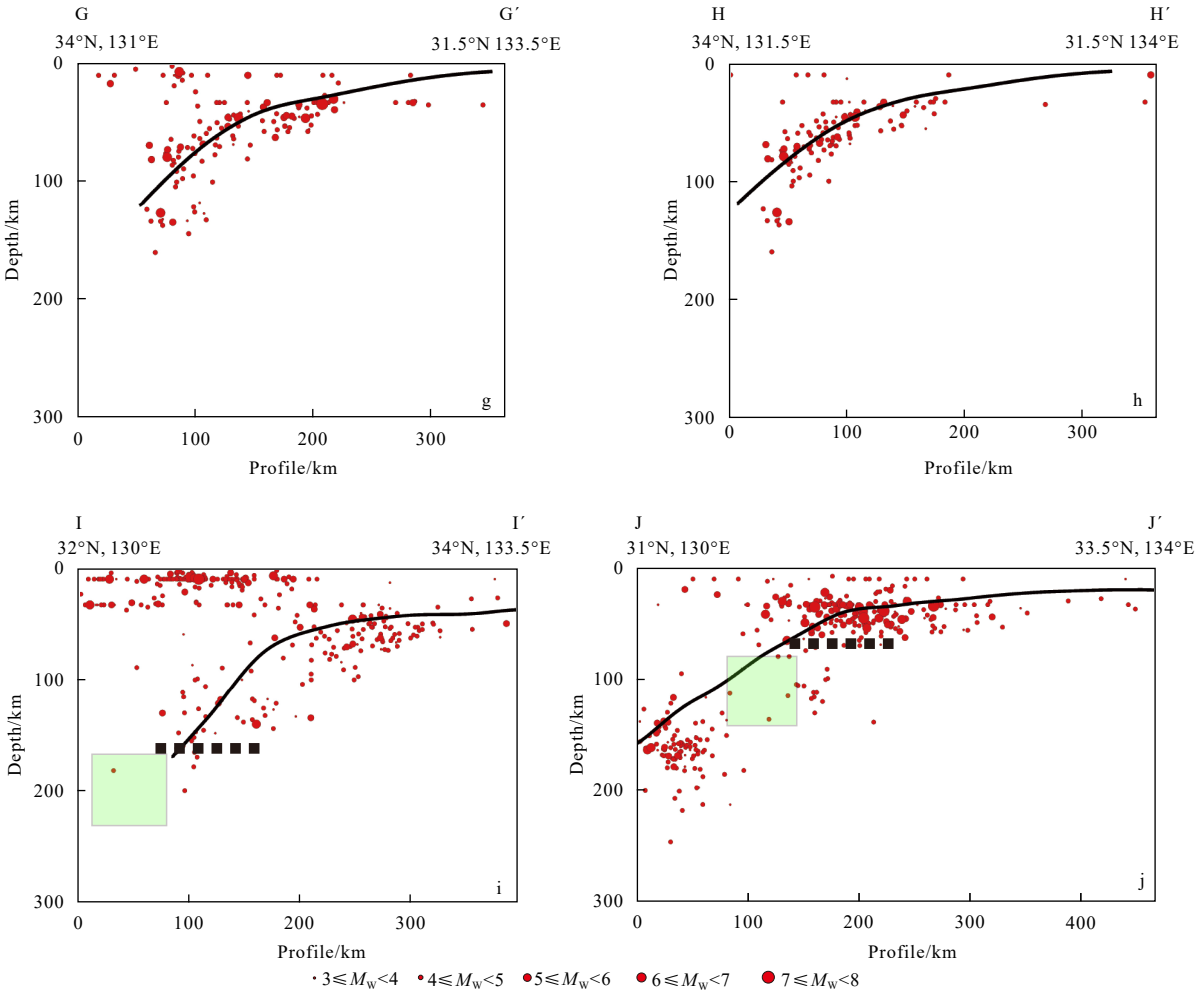


**Fig. 5.** Distributions of earthquakes along typical cross-sections. The cross-sections are 100 km wide. The thick black lines mark the upper boundary of the subducting slab (Slab 1.0). The light green rectangles mark the seismic gaps. The black dotted line represents the location of the KPR.

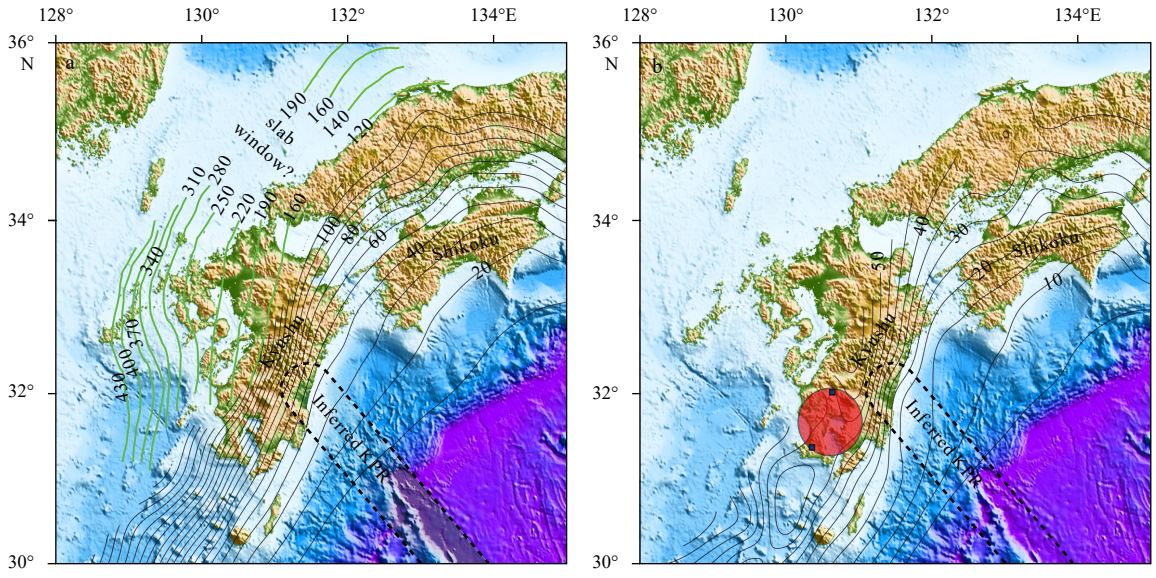


**Fig. 6.** Morphology of the upper boundary of the subducting PS slab beneath southwest Japan. a. Depth of the upper boundary of the subducting PS slab. The green lines denote the upper boundary of the subducting PS slab estimated from the teleseismic tomography (Zhao et al., 2012). b. Subduction angles of the subducting PS slab. The light pink ellipse shows a sudden change in the subduction angle that may be related to the subduction of the KPR.

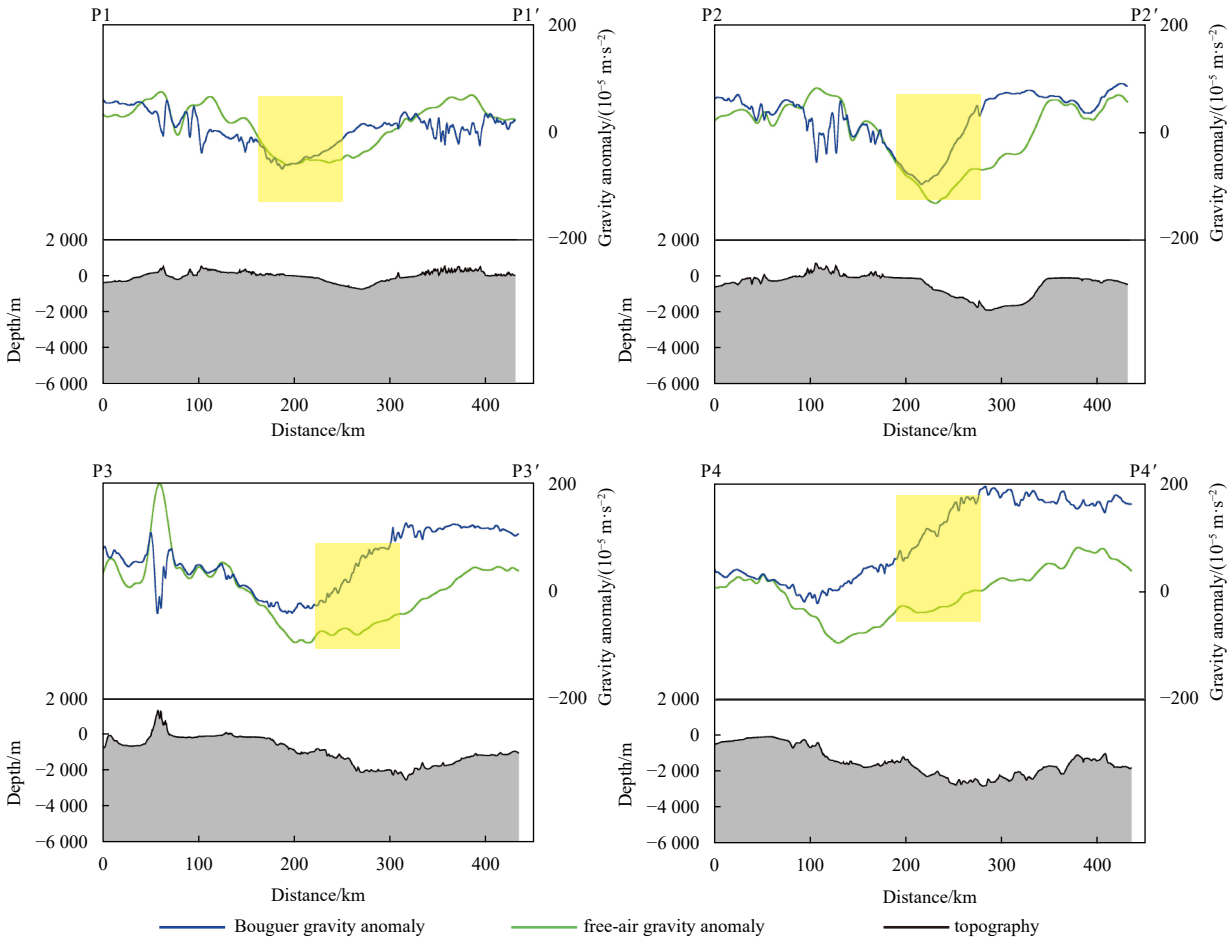


**Fig. 7.** Comprehensive geophysical (Bouguer anomaly, free-air anomaly, and topography) sections perpendicular to the inferred KPR (see Fig. 2a for line location). The light yellow rectangles represent the location of the inferred KPR.

The geophysical cross-sections perpendicular to the extension of the inferred KPR suggest that the prolonged area of buoyant KPR shows lower free-air anomalies and Bouguer anomalies compared to the Shikoku forearc (Fig. 7). Furthermore, a negative Bouguer anomaly depression is observed in a prolonged area of KPR, southeast of the Miyazaki Plain, corresponding to the negative free-air anomaly depression. The Bouguer gravity anomaly includes the influence of various geological bodies and structures that deviate from the normal density distribution in the crust, and also includes the effect of loss or surplus relative to the mass of the mantle due to the fluctuations in Moho depth. The minimum negative Bouguer anomaly depression off the Miyazaki Plain may indicate that this area represents the deep Moho, which is confirmed by the Moho topography (Oda and Ushio, 2007).

However, the gravity anomaly in the area marked with an ellipse in Fig. 2 is much lower than that in other prolonged areas of KPR. Thus, in addition to the influence of the depth variation of the Moho, the Bouguer anomaly must be affected by other factors. The buoyant KPR composed of light volcanic rocks is subducting beneath the eastern Kyushu, and the upper mantle of the region must become low density (Oda and Ushio, 2007). Recent studies have shown that the subduction of the KPR has important influences on the deformation and serpentinization in the forearc mantle wedge within the Kyushu subduction zone (Ichikawa, 1997; Xia et al., 2008; Abe et al., 2011; Xia et al., 2015). The water content in the forearc mantle wedge is relatively high, and the wedge has been subjected to different degrees of serpentinization, which may also contribute to the lower Bouguer anomaly in this area.

Comparative studies demonstrate that more earthquakes occur in the Kyushu subduction zone corresponding to the KPR than in the Shikoku subduction zone. In addition, all earthquakes with a magnitude greater than 7 that have occurred in the Kyushu forearc since the 1960s were concentrated in the area overlying the inferred area of the subducting KPR (Fig. 3). The relatively high water content and high degree of serpentinization in the Kyushu forearc (Abe et al., 2011, 2013; Xia et al., 2015) corresponding to the KPR should have provided a ductile environment for weak seismicity, but this is inconsistent with current seismic coupling. The spatial distribution of the earthquakes is closely related to the seafloor relief (Shi, 1998; Kong et al., 2018). Bathymetry highs entering the subduction zone, such as seamounts and aseismic ridges, can affect the magnitude, frequency and spatial distribution of the earthquakes by adjusting the coupling between the subduction plate and the overlying plate (Kelleher and McCann, 1976; Scholz and Small, 1997; Watts et al., 2010; Yamamoto et al., 2014). Thus, the relatively high number of earthquakes near the KPR indicates that the subduction of the KPR has a significant impact on the formation of earthquakes in

this region. The concentration of thrust-type intermediate-magnitude earthquakes in the Kyushu forearc suggests the potential for locally large tectonic stresses along the contact zone between the subducting ridge and the base of the overriding plate, which is often conducive to a high moment release (Park et al., 2009).

The inhomogeneity of the earthquake distribution reveals geometrical differences of the subducting slab beneath the Kyushu and Shikoku. The PS slab shows a sudden change in its subduction depth from 20–50 km under Shikoku to 50–300 km under northern Kyushu. The dip angle of the PS slab changes from 10°–25° under Shikoku to 25°–65° under northern Kyushu (Fig. 6). The different ages of the oceanic crust between the West Philippine Basin and the Shikoku Basin can be responsible for the changes in subduction depth and dip angle of the subducting PS slab to a certain extent, but this disparity cannot explain the difference in the subduction depth and dip angle of the subducting slab beneath northern Kyushu and Shikoku, because the diving Shikoku Basin is below both. Thus, we consider it more likely that the buoyant KPR, with a large volume of low-density sediments, was responsible for the differences of the subduction depth and dip angle of the subducting PS slab between northern Kyushu and Shikoku.

### 4.2 *Slab tear: Related to subduction of the KPR?*

Special tectonic settings, such as young subducting slabs, gentle dip angles, high geothermal gradients, and slab windows, can lead to the dehydration and melting of hydrous minerals (Defant and Drummond, 1990; Gutscher et al., 2000; Yogodzinski et al., 2001; Chen et al., 2012). Adakites or adakite-like lavas have been discovered in the Philippines (Sajona, 1993), the northern part of the Tonga Trench (Falloon et al., 2008), the Central American arc (Bourdon et al., 2002; Defant et al., 1992; Reagan and Gill, 1989), and the Kamchatka Peninsula (Kepezhinskas et al., 1996, 1997). Each region mentioned above displays a slab window, and all of these cases exhibit similar tectonic settings (a bathymetric high subducts with the slab) to that of southwest Japan. The collision of bathymetric highs atop the seafloor with the trench has been linked to tearing of the subducting slab (Bautista et al., 2001; Mason et al., 2010). Thus, the adakites in northeast Kyushu and southwest Honshu were attributable to the melting of the subducted PSP. Furthermore, high-resolution seismic tomography confirms that the high P-wave velocity anomaly is interrupted by a low-velocity anomaly zone beneath Kyushu and western Honshu (Fig. 8), and it is considered that this was the result of the formation of the slab window which is related to the subduction of the buoyant KPR and the motion change of the PSP (Zhao et al., 2012; Huang et al., 2013; Cao et al., 2014).

However, the slab window beneath northeast Kyushu and southwest Honshu cannot explain the adakites and high-magnesian andesites found in southwestern Kyushu. Seismic gaps were found at depths of 200 km and 100 km west of the prolonged area of KPR along cross-sections I–I′ and J–J′ parallel to the strike of the subduction zone, respectively. Seismic gaps are also reflected in sections A–A′, B–B′, and C–C′ at a depth of 80–100 km (Fig. 5). These are similar to the seismic gaps observed beneath the North Andean margin and the Savu Sea, and are thought to be related to the subduction of the Carnegie Ridge and Scott Plateau (Gutscher et al., 1999; Ely and Sandiford, 2010), respectively. The subduction angle change dramatically beneath southern Kyushu. Low velocity anomalies were observed west of Kyushu Island based on the seismic tomography (Sadeghi et al., 2000; Zhao et al., 2000), and it is considered that this was related to the upwelling of hot mantle. Low-sulfidation epithermal gold deposits and high-sulfidation gold deposits were discovered in southwest Kyushu, and Cooke et al. (2005) believed that the porphyry deposits may have formed in southwest Kyushu but that the degree of uplift and exhumation was not sufficient to expose the porphyry system in this area. The adakite magmas formed by partial melting of the oceanic crust have high copper and gold contents, which are conducive to the formation of porphyry copper and gold deposits (Cooke et al., 2005; Sun et al., 2010). Therefore, the gold deposits in southwest Kyushu may be the result of the partial melting of the subducting PSP related to KPR subduction. In summary, the seismic gaps, subducted slab morphology, low velocity anomalies, and distribution of adakites and gold deposits in southwest Kyushu indicate that slab tear may have occurred beneath southwest Kyushu along the west side of the KPR.

The young (<30 Ma), warm Shikoku Basin to the east of the KPR is subducting beneath northern Kyushu, while the old (>45 Ma), cold and dense West Philippine Basin to the west of the KPR is subducting beneath southern Kyushu (Fig. 1). Differences in the lithosphere density produce different slab pull forces, which can be responsible for slab tear. However, if the difference in the lithosphere density between the Shikoku Basin and the West Philippine Basin is the only factor causing slab tear, then theoretically, there will be only one tear or slab window under Kyushu. However, the large-scale slab window that exists under Kyushu cannot be supported by current geophysical and geochemical data. Therefore, we believe that the KPR plays an important role in the slab tear, which favors a two-tear model (Fig. 9).

As a bathymetric high lies on the PSP, the KPR with excess mass may be relatively buoyant, while the cooled subducting slab segments on either side boast a higher density and a larger slab pull than those of the ridge (Fig. 9). The buoyancy difference between the KPR and the slab segments on both sides gradually increases with depth, leading us to speculate that tears occur along the flanks of the KPR. Then, hot mantle material surges through these cracks, and the slab edges are heated and melted to form adakitic magmas (Yogodzinski et al., 2001). These adakitic magmas then interact with the peridotite of the overlying mantle wedge to form high-magnesian andesites, which explains the coexistence of high-magnesian andesites and adakites.

## 5 Conclusions

In this paper, the gravity anomalies and seismicity of the Kyushu and Shikoku areas of southwest Japan are described in detail. By comparing the geological and geophysical differences between Shikoku subduction zone and Kyushu subduction zone where the KPR subducts, the tectonic significance of KPR subduction under Kyushu is discussed. The principal conclusions are as follows.

(1) Significant negative free-air and Bouguer gravity anomalies are observed in a prolonged area of KPR, southeast of the Miyazaki Plain, indicating that this is where the KPR overlaps the overriding plate. The gravity anomaly in this area is much lower than that in other areas where the inferred KPR extends, suggesting the subduction of the buoyant KPR may cause the lower mantle density to decrease.

(2) The CMT mechanism of earthquakes shows that the stress is concentrated in the accumulated crust beneath the Kyushu forearc where the KPR subducts, and the shallow thrusting events in the obducting plate are caused by the KPR subduction. More earthquakes have occurred in the Hyuga-nada where the KPR subducts than in Shikoku forearc and other areas in the Ky-

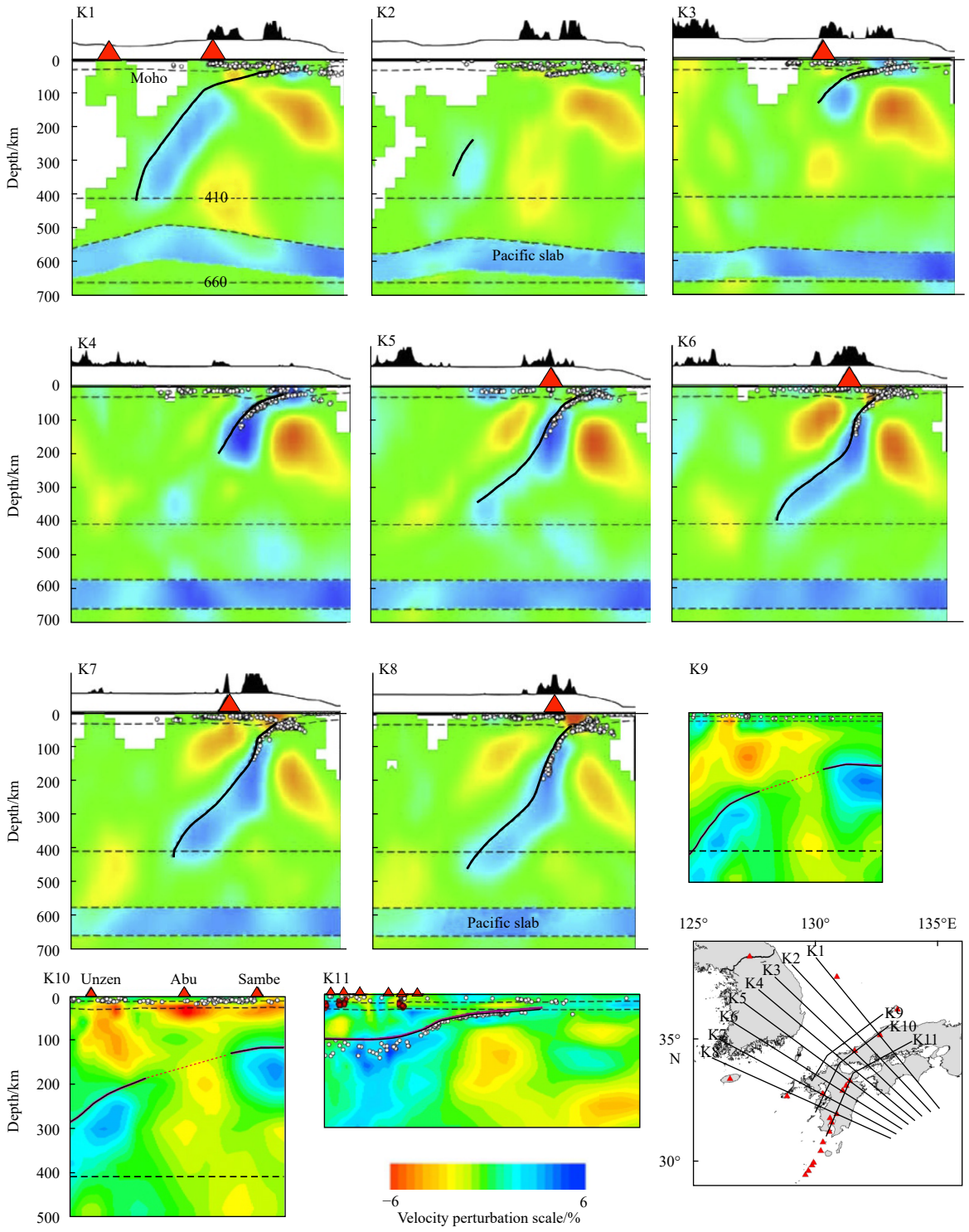


**Fig. 8.** Vertical P-wave tomography cross-sections along the profiles shown on the inset map (modified from Huang et al., 2013; Cao et al., 2014). Red and blue colors denote lower and higher velocities, respectively. The velocity perturbation scale (%) is shown at the bottom. The red triangles denote active arc volcanoes. The red broken lines in K9 and K10 represent the discontinuity or gap in the high-velocity zone. The two dashed lines in each cross-section represent the 410 km and 660 km discontinuities. The white dots denote seismicity that occurred within a 20 km width of each profile.

ushu forearc, indicating that the subduction of the KPR enhances the local coupling between the subducting and overriding plates.

(3) The buoyant KPR, with a large volume of low-density sediments, was responsible for the differences of the subduction depth and dip angle of the subducting PS slab between northern Kyushu and Shikoku. The seismic gaps and the sudden change of the dipping angle of the subducting PS slab indicate that slab tear may have occurred along the west side of the KPR beneath southwest Kyushu, which provides a reasonable explanation for the

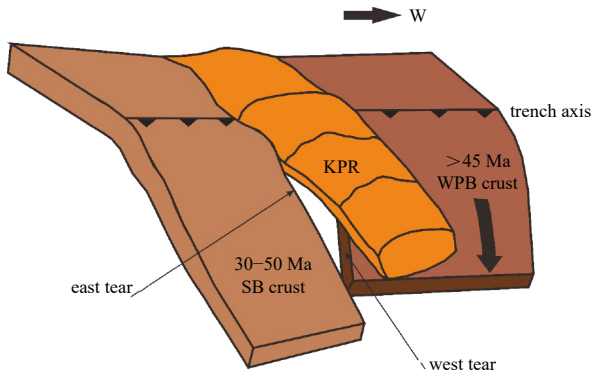


**Fig. 9.** 3-D view of the two-tear model for the subducting KPR. See Fig. 1 for abbreviations.

low velocity anomalies, and the distribution of adakites and gold deposits in southwest Kyushu. A two-tear model was proposed, and the subduction of the buoyant KPR was believed to play an important role in the slab tear.

***Acknowledgements***

We are grateful to Q. Yan for his help in geology and geochemistry interpretation. The figures in this paper are produced using the GMT software (Wessel et al., 2013).

**References**

Abe Y, Ohkura T, Hirahara K, et al. 2011. Water transportation through the Philippine Sea slab subducting beneath the central Kyushu region, Japan, as derived from receiver function analyses. Geophysical Research Letters, 38(23): L23305

Abe Y, Ohkura T, Hirahara K, et al. 2013. Along-arc variation in water distribution in the uppermost mantle beneath Kyushu, Japan, as derived from receiver function analyses. Journal of Geophysical Research: Solid Earth, 118(7): 3540–3556, doi: 10.1002/jgrb.50257

Amante C, Eakins B W. 2009. ETOPO1 1 arc-minute global relief model: procedures, data sources and analysis. NOAA Technical Memorandum NESDIS NGDC-24. National Geophysical Data Center, NOAA

Bautista B C, Bautista M L P, Oike K, et al. 2001. A new insight on the geometry of subducting slabs in northern Luzon, Philippines. Tectonophysics, 339(3–4): 279–310

Bourdon E, Eissen J P, Monzier M, et al. 2002. Adakite-like lavas from Antisana volcano (Ecuador): Evidence for slab melt metasomatism beneath Andean northern volcanic zone. Journal of Petrology, 43(2): 199–217, doi: 10.1093/petrology/43.2.199

Cao Lingmin, Wang Zhi, Wu Shiguo, et al. 2014. A new model of slab tear of the subducting Philippine Sea Plate associated with Kyushu-Palau Ridge subduction. Tectonophysics, 636: 158–169, doi: 10.1016/j.tecto.2014.08.012

Castle J C, Creager K C. 1998. Topography of the 660-km seismic discontinuity beneath Izu-Bonin: Implications for tectonic history and slab deformation. Journal of Geophysical Research: Solid Earth, 103(B6): 12511–12527, doi: 10.1029/98JB00503

Castle J C, Creager K C. 1999. A steeply dipping discontinuity in the lower mantle beneath Izu-Bonin. Journal of Geophysical Research: Solid Earth, 104(B4): 7279–7292, doi: 10.1029/1999JB900011

Chen Yuxiao, Xia Xiaohong, Song Shuguang. 2012. Petrogenesis of Aoyougou high-silica adakite in the North Qilian orogen, NW China: evidence for decompression melting of oceanic slab. Chinese Science Bulletin, 57(18): 2289–2301, doi: 10.1007/s11434-012-5069-3

Chen Ping, Zheng Yanpeng, Liu Baohua. 2014. Geophysical features of the Nankai Trough subduction zone and their dynamic significance. Marine Geology & Quaternary Geology (in Chinese), 34(6): 153–160

Cooke D R, Hollings P, Walshe J L. 2005. Giant porphyry deposits: characteristics, distribution, and tectonic controls. Economic Geology, 100(5): 801–818, doi: 10.2113/gsecongeo.100.5.801

Cooke D R, Simmons S F. 2000. Characteristics and genesis of epithermal gold deposits. Reviews in Economic Geology, 13: 221–244

Cosca M, Arculus R J, Pearce J, et al. 1998. $^{40}Ar/^{39}Ar$ and K–Ar geochronological age constraints for the inception and early evolution of the Izu-Bonin-Mariana arc system. Island Arc, 7(3): 579–595, doi: 10.1111/j.1440-1738.1998.00211.x

Das S, Watts A B. 2009. Effect of subducting seafloor topography on the rupture characteristics of great subduction zone earthquakes. In: Lallemand S, Funiciello F, eds. Subduction Zone Geodynamics. Berlin, Heidelberg: Springer, 103–108

Defant M J, Drummond M S. 1990. Derivation of some modern arc magmas by melting of young subducted lithosphere. Nature, 347(6294): 662–665, doi: 10.1038/347662a0

Defant M J, Jackson T E, Drummond M S, et al. 1992. The geochemistry of young volcanism throughout western Panama and southeastern Costa Rica: An overview. Journal of the Geological Society, 149(4): 569–579, doi: 10.1144/gsjgs.149.4.0569

Defant M J, Sherman S, Maury R C, et al. 2001. The geology, petrology, and petrogenesis of Saba Island, Lesser Antilles. Journal of Volcanology and Geothermal Research, 107(1–3): 87–111

DeMets C, Gordon R G, Argus D F. 2010. Geologically current plate motions. Geophysical Journal International, 181(1): 1–80, doi: 10.1111/j.1365-246X.2009.04491.x

Deschamps A, Lallemand S. 2002. The West Philippine Basin: An Eocene to early Oligocene back arc basin opened between two opposed subduction zones. Journal of Geophysical Research: Solid Earth, 107(B12): EPM 1-1–EPM 1-24, doi: 10.1029/2001JB001706

Dziewonski A M, Chou T A, Woodhouse J H, et al. 1981. Determination of earthquake source parameters from waveform data for studies of global and regional seismicity. Journal of Geophysical Research: Solid Earth, 86(B4): 2825–2585, doi: 10.1029/JB086iB04p02825

Ekström G, Nettles M, Dziewoński A M. 2012. The global CMT project 2004–2010: Centroid-moment tensors for 13,017 earthquakes. Physics of the Earth and Planetary Interiors, 200–201: 1–9

Ely K S, Sandiford M. 2010. Seismic response to slab rupture and variation in lithospheric structure beneath the Savu Sea, Indonesia. Tectonophysics, 483(1–2): 112–124

Falloon T J, Danyushevsky L V, Crawford A J, et al. 2008. Boninites and adakites from the northern termination of the Tonga trench: Implications for Adakite Petrogenesis. Journal of Petrology, 49(4): 697–715

Fan Jianke, Wu Shiguo, Spence G. 2015. Tomographic evidence for a slab tear induced by fossil ridge subduction at Manila Trench, South China Sea. International Geology Review, 57(5–8): 998–1013

Fan Jianke, Zhao Dapeng, Dong Dongdong. 2016. Subduction of a buoyant plateau at the Manila Trench: Tomographic evidence and geodynamic implications. Geochemistry, Geophysics, Geosystems, 17(2): 571–586, doi: 10.1002/2015GC006201

Gurnis M, Hall C, Lavier L. 2004. Evolving force balance during incipient subduction. Geochemistry, Geophysics, Geosystems, 5(7): Q07001

Gutscher M A, Malavieille J, Lallemand S, et al. 1999. Tectonic segmentation of the North Andean margin: Impact of the Carnegie Ridge collision. Earth and Planetary Science Letters, 168(3–4): 255–270

Gutscher M A, Maury R, Eissen J P, et al. 2000. Can slab melting be caused by flat subduction?. Geology, 28(6): 535–538, doi: 10.1130/0091-7613(2000)28<535:CSMBCB>2.0.CO;2

Hall R. 2002. Cenozoic geological and plate tectonic evolution of SE Asia and the SW Pacific: Computer-based reconstructions, model and animations. Journal of Asian Earth Sciences, 20(4): 353–431, doi: 10.1016/S1367-9120(01)00069-4

Hall R, Ali J R, Anderson C D. 1995a. Cenozoic motion of the Philippine Sea Plate: palaeomagnetic evidence from eastern Indonesia. Tectonics, 14(5): 1117–1132, doi: 10.1029/95TC01694
Hall R, Ali J R, Anderson C D, et al. 1995b. Origin and motion history of the Philippine Sea Plate. Tectonophysics, 251(1–4): 229–250
Hall R, Fuller M, Ali J R, et al. 1995c. The Philippine Sea Plate: Magnetism and reconstructions. In: Taylor B, Natland J, eds. Active Margins and Marginal Basins of the Western Pacific. Washington, D C: American Geophysical Union, 371–403
Hall C E, Gurnis M, Sdrolias M, et al. 2003. Catastrophic initiation of subduction following forced convergence across fracture zones. Earth and Planetary Science Letters, 212(1–2): 15–30
Haraguchi S, Ishii T, Kimura J I, et al. 2003. Formation of tonalite from basaltic magma at the Komahashi-Daini Seamount, northern Kyushu-Palau Ridge in the Philippine Sea, and growth of Izu-Ogasawara (Bonin)-Mariana arc crust. Contributions to Mineralogy and Petrology, 145(2): 151–168, doi: 10.1007/s00410-002-0433-y
Hayes G P, Wald D J, Johnson R L. 2012. Slab1.0: A three-dimensional model of global subduction zone geometries. Journal of Geophysical Research, 117(B1): B01302
Hedenquist J W, Matsuhisa Y, Izawa E, et al. 1994. Geology, geochemistry, and origin of high sulfidation Cu-Au mineralization in the Nansatsu District, Japan. Economic Geology, 89(1): 1–30, doi: 10.2113/gsecongeo.89.1.1
Huang Zhouchuan, Zhao Dapeng, Hasegawa A, et al. 2013. Aseismic deep subduction of the Philippine Sea plate and slab window. Journal of Asian Earth Sciences, 75: 82–94, doi: 10.1016/j.jseaes.2013.07.002
Ichikawa G. 1997. Ocean bottom seismographic experiment to study crustal structure in Hyuga-nada [dissertation]. Sapporo: University of Hokkaido (in Japanese)
Ishihara T, Koda K. 2007. Variation of crustal thickness in the Philippine Sea deduced from three-dimensional gravity modeling. Island Arc, 16(3): 322–337, doi: 10.1111/j.1440-1738.2007.00593.x
Ishizuka O, Taylor R N, Yuasa M, et al. 2011. Making and breaking an island arc: A new perspective from the Oligocene Kyushu-Palau arc, Philippine Sea. Geochemistry, Geophysics, Geosystems, 12(5): Q05005
Izawa E, Urashima Y, Ibaraki K, et al. 1990. The Hishikari gold deposit: High-grade epithermal veins in Quaternary volcanics of southern Kyushu, Japan. Journal of Geochemical Exploration, 36(1–3): 1–56
Kakubuchi S, Nagao T, Nagao K. 2000. K-Ar ages and magmatic history of the Abu Monogenetic Volcano Group, southwest Japan. Japanese Magazine of Mineralogical and Petrological Sciences (in Japanese), 29(5): 191–198, doi: 10.2465/gkk.29.191
Karig D E. 1972. Remnant arcs. GSA Bulletin, 83(4): 1057–1068, doi: 10.1130/0016-7606(1972)83[1057:RA]2.0.CO;2
Karig D E, Ingle J C Jr. 1975. Initial Reports of the Deep Sea Drilling Project. Washington, US: Government Printing Office, 191–274
Kelleher J, McCann W. 1976. Buoyant zones, great earthquakes, and unstable boundaries of subduction. Journal of Geophysical Research, 81(26): 4885–4896, doi: 10.1029/JB081i026p04885
Kepezhinskas P, Defant M J, Drummond M S. 1996. Progressive enrichment of island arc mantle by melt-peridotite interaction inferred from Kamchatka xenoliths. Geochimica et Cosmochimica Acta, 60(7): 1217–1229, doi: 10.1016/0016-7037(96)00001-4
Kepezhinskas P, McDermott F, Defant M J, et al. 1997. Trace element and Sr-Nd-Pb isotopic constraints on a three-component model of Kamchatka Arc petrogenesis. Geochimica et Cosmochimica Acta, 61(3): 577–600, doi: 10.1016/S0016-7037(96)00349-3
Kimura G. 1996. Collision orogeny at arc-arc junctions in the Japanese islands. Island Arc, 5(3): 262–275, doi: 10.1111/j.1440-1738.1996.tb00031.x
Kimura J I, Kunikiyo T, Osaka I, et al. 2003. Late Cenozoic volcanic activity in the Chugoku area, southwest Japan arc during back-arc basin opening and reinitiation of subduction. Island Arc, 12(1): 22–45, doi: 10.1046/j.1440-1738.2003.00377.x
Kodama K, Tashiro H, Takeuchi T. 1995. Quaternary counterclockwise rotation of south Kyushu, southwest Japan. Geology, 23(9): 823–826, doi: 10.1130/0091-7613(1995)023<0823:QCROSK>2.3.CO;2
Kong Xiangchao, Li Sanzhong, Wang Yongming, et al. 2017. Triggering causes of earthquakes along the Izu-Bonin-Mariana subduction zone. Marine Geology & Quaternary Geology (in Chinese), 37(4): 83–97
Kong Xiangchao, Li Sanzhong, Wang Yongming, et al. 2018. Causes of earthquake spatial distribution beneath the Izu-Bonin-Mariana Arc. Journal of Asian Earth Sciences, 151: 90–100, doi: 10.1016/j.jseaes.2017.10.015
Lallemand S. 2016. Philippine Sea Plate inception, evolution, and consumption with special emphasis on the early stages of Izu-Bonin-Mariana subduction. Progress in Earth and Planetary Science, 3(1): 15, doi: 10.1186/s40645-016-0085-6
Mahony S H, Wallace L M, Miyoshi M, et al. 2011. Volcano-tectonic interactions during rapid plate-boundary evolution in the Kyushu region, SW Japan. GSA Bulletin, 123(11–12): 2201–2223
Mason W G, Moresi L, Betts P G, et al. 2010. Three-dimensional numerical models of the influence of a buoyant oceanic plateau on subduction zones. Tectonophysics, 483(1–2): 71–79
Miller M S, Kennett B L N, Lister G S. 2004. Imaging changes in morphology, geometry, and physical properties of the subducting Pacific plate along the Izu-Bonin-Mariana arc. Earth and Planetary Science Letters, 224(3–4): 363–370
Morris P A. 1995. Slab melting as an explanation of Quaternary volcanism and aseismicity in southwest Japan. Geology, 23(5): 395–398, doi: 10.1130/0091-7613(1995)023<0395:SMAAEO>2.3.CO;2
Mungall J E. 2002. Roasting the mantle: slab melting and the genesis of major Au and Au-rich Cu deposits. Geology, 30(10): 915–918, doi: 10.1130/0091-7613(2002)030<0915:RTMSMA>2.0.CO;2
Nagaoka S. 1986. The landform evolution of Late Pleistocene in the Miyazaki Plain, South Kyushu, Japan. The Quaternary Research, 25(3): 139–163, doi: 10.4116/jaqua.25.139
Nakada M, Tahara M, Shimizu H, et al. 2002. Late Pleistocene crustal uplift and gravity anomaly in the eastern part of Kyushu, Japan, and its geophysical implications. Tectonophysics, 351(4): 263–283, doi: 10.1016/S0040-1951(02)00161-0
Nishimura S, Ando M, Miyazaki S. 1999. Inter-plate coupling along the Nankai Trough and southeastward motion along southern part of Kyushu. Zisin (Journal of the Seismological Society of Japan. 2nd ser.), 51(4): 443–456, doi: 10.4294/zisin1948.51.4_443
Nishizawa A, Kaneda K, Katagiri Y, et al. 2007. Variation in crustal structure along the Kyushu-Palau Ridge at 15–21°N on the Philippine Sea plate based on seismic refraction profiles. Earth, Planets and Space, 59(6): e17–e20, doi: 10.1186/BF03352711
Nishizawa A, Kaneda K, Oikawa M. 2009. Seismic structure of the northern end of the Ryukyu Trench subduction zone, southeast of Kyushu, Japan. Earth, Planets and Space, 61(8): e37–e40, doi: 10.1186/BF03352942
Oda H, Ushio T. 2007. Topography of the Moho and Conrad discontinuities in the Kyushu district, Southwest Japan. Journal of Seismology, 11(2): 221–233, doi: 10.1007/s10950-007-9049-z
Okino K, Ohara Y, Kasuga S, et al. 1999. The Philippine Sea: new survey results reveal the structure and the history of the marginal basins. Geophysical Research Letters, 26(15): 2287–2290, doi: 10.1029/1999GL900537
Okino K, Shimakawa Y, Nagaoka S. 1994. Evolution of the Shikoku Basin. Journal of Geomagnetism & Geoelectricity, 46(6): 463–479
Oyarzun R, Márquez A, Lillo J, et al. 2001. Giant versus small porphyry copper deposits of Cenozoic age in northern Chile: Adakitic versus normal calc-alkaline magmatism. Mineralium Deposita, 36(8): 794–798, doi: 10.1007/s001260100205
Park J O, Hori T, Kaneda Y. 2009. Seismotectonic implications of the Kyushu-Palau ridge subducting beneath the westernmost Nankai forearc. Earth, Planets and Space, 61(8): 1013–1018, doi: 10.1186/BF03352951
Peacock S M, Rushmer T, Thompson A B. 1994. Partial melting of subducting oceanic crust. Earth and Planetary Science Letters, 121(1–2): 227–244

Reagan M K, Gill J B. 1989. Coexisting calcalkaline and high-niobium basalts from turrialba volcano, Costa Rica: Implications for residual titanates in arc magma sources. Journal of Geophysical Research, 94(B4): 4619–4633, doi: 10.1029/JB094iB04p04619

Sadeghi H, Suzuki S, Takenaka H. 2000. Tomographic low-velocity anomalies in the uppermost mantle around the northeastern edge of Okinawa trough, the backarc of Kyushu. Geophysical Research Letters, 27(2): 277–280, doi: 10.1029/1999GL008385

Sajona F G, Maury R C. 1998. Association of adakites with gold and copper mineralization in the philippines. Comptes Rendus De L'Académie Des Sciences-Series IIA-Earth and Planetary Science, 326(1): 27–34

Sajona F G, Maury R C, Bellon H, et al. 1993. Initiation of subduction and the generation of slab melts in western and eastern Mindanao, Philippines. Geology, 21(11): 1007–1010, doi: 10.1130/0091-7613(1993)021<1007:IOSATG>2.3.CO;2

Sandwell D T, Müller R D, Smith W H F, et al. 2014. New global marine gravity model from CryoSat-2 and Jason-1 reveals buried tectonic structure. Science, 346(6205): 65–67, doi: 10.1126/science.1258213

Scholz C H, Small C. 1997. The effect of seamount subduction on seismic coupling. Geology, 25(6): 487–490, doi: 10.1130/0091-7613(1997)025<0487:TEOSSO>2.3.CO;2

Sdrolias M, Roest W R, Müller R D. 2004. An expression of Philippine Sea plate rotation: The Parece Vela and Shikoku basins. Tectonophysics, 394(1–2): 69–86

Sella G F, Dixon T H, Mao Ailin. 2002. REVEL: A model for recent plate velocities from space geodesy. Journal of Geophysical Research: Solid Earth, 107(B4): ETG 11-1–ETG 11-30, doi: 10.1029/2000JB000033

Seno T, Maruyama S. 1984. Paleogeographic reconstruction and origin of the Philippine Sea. Tectonophysics, 102(1–4): 53–84

Shi Xuejian. 1998. Spatial differences of the earthquake distribution along the island-arcs in the western Pacific and their causes. Seismology and Geology (in Chinese), 20(4): 399–404

Shimoyama S, Kinoshita H, Miyahara M, et al. 1999. Mode of vertical crustal movements during the late quaternary in Kyushu, Japan, deduced from heights of ancient shorelines. Tectonophysics, 302(1–2): 9–22

Smith W H F, Sandwell D T. 1997. Global sea floor topography from satellite altimetry and ship depth soundings. Science, 277(5334): 1956–1962, doi: 10.1126/science.277.5334.1956

Sugimoto T, Shibata T, Yoshikawa M, et al. 2006. Sr-Nd-Pb isotopic and major and trace element compositions of the Yufu-Tsurumi volcanic rocks: implications for the magma genesis of the Yufu-Tsurumi volcanoes, northeast Kyushu, Japan. Journal of Mineralogical and Petrological Sciences, 101(5): 270–275, doi: 10.2465/jmps.101.270

Sun Weidong, Ling Mingxing, Yang Xiaoyong, et al. 2010. Ridge subduction and porphyry copper-gold mineralization: An overview. Science China Earth Sciences, 53(4): 475–484, doi: 10.1007/s11430-010-0024-0

Sun Weidong, Zhang Hong, Ling Mingxing, et al. 2011. The genetic association of adakites and Cu-Au ore deposits. International Geology Review, 53(5–6): 691–703

Tahara M, Uehira K, Shimizu H, et al. 2008. Seismic velocity structure around the Hyuganada region, Southwest Japan, derived from seismic tomography using land and OBS data and its implications for interplate coupling and vertical crustal uplift. Physics of the Earth and Planetary Interiors, 167(1–2): 19–33

Thiéblemont D, Stein G, Lescuyer J L. 1997. Epithermal and porphyry deposits: The adakite connection. Comptes Rendus De L'Académie Des Sciences Series IIA Earth and Planetary Science, 325(2): 103–109

Tozer B, Sandwell D T, Smith W H F, et al. 2019. Global bathymetry and topography at 15 arc sec: SRTM15+. Earth and Space Science, 6(10): 1847–1864, doi: 10.1029/2019EA000658

Wang Kelin, Wada I, Ishikawa Y. 2004. Stresses in the subducting slab beneath southwest Japan and relation with plate geometry, tectonic forces, slab dehydration, and damaging earthquakes. Journal of Geophysical Research: Solid Earth, 109(B8): B08304

Watts A B, Koppers A A P, Robinson D P. 2010. Seamount subduction and earthquakes. Oceanography, 23(1): 166–173, doi: 10.5670/oceanog.2010.68

Wessel P, Smith W H F, Scharroo R, et al. 2013. Generic mapping tools: improved version released. Eos, Transactions American Geophysical Union, 94(45): 409–410

Xia Shaohong, Sun Jinlong, Huang Haibo. 2015. Degree of serpentinization in the forearc mantle wedge of Kyushu subduction zone: Quantitative evaluations from seismic velocity. Marine Geophysical Research, 36(2–3): 101–112

Xia Chenglong, Zheng Yanpeng, Dong Dongdong, et al. 2017. Characteristics of magnetic lineations and reconstruction of seafloor spreading processes of the Philippine Sea Basin since 61 Ma. Marine Geology and Quaternary Geology (in Chinese), 37(1): 30–40

Xia Shaohong, Zhao Dapeng, Qiu Xuelin. 2008. Tomographic evidence for the subducting oceanic crust and forearc mantle serpentinization under Kyushu, Japan. Tectonophysics, 449(1–4): 85–96

Yamamoto Y, Obana K, Takahashi T, et al. 2014. Seismicity and structural heterogeneities around the western Nankai Trough subduction zone, southwestern Japan. Earth and Planetary Science Letters, 396: 34–45, doi: 10.1016/j.epsl.2014.04.006

Yan Quanshu, Shi Xuefa. 2011. Geological comparative studies of Japan arc system and Kyushu-Palau arc. Acta Oceanologica Sinica, 30(4): 107–121, doi: 10.1007/s13131-011-0134-3

Yan Quanshu, Shi Xuefa. 2014. Geological effects of aseismic ridges or seamount chains subduction on the supra-subduction zone. Haiyang Xuebao (in Chinese), 36(5): 107–123

Yogodzinski G M, Lees J M, Churikova T G, et al. 2001. Geochemical evidence for the melting of subducting oceanic lithosphere at plate edges. Nature, 409(6819): 500–504, doi: 10.1038/35054039

Zang Shaoxian, Ning Jieyuan. 1996. Study on the subduction zone in western pacific and its implication for the geodynamics. Acta Geophysica Sinica (in Chinese), 39(2): 188–202

Zhang Jie, Li Jiabiao, Ding Weiwei. 2012. Reviews of the study on crustal structure and evolution of the Kyushu-Palau ridge. Advances in Marine Science (in Chinese), 30(4): 595–607

Zhao Dapeng, Asamori K, Iwamori H. 2000. Seismic structure and magmatism of the young Kyushu subduction zone. Geophysical Research Letters, 27(14): 2057–2060, doi: 10.1029/2000GL011512

Zhao Dapeng, Yanada T, Hasegawa A, et al. 2012. Imaging the subducting slabs and mantle upwelling under the Japan islands. Geophysical Journal International, 190(2): 816–828, doi: 10.1111/j.1365-246X.2012.05550.x